# Elimination of Ascorbic Acid and Sensitive Detection of Uric Acid at the MnO$_2$ Nanorods /Graphene-based Modified Electrode

*Zong-hua Wang[1,*], Jie Tang[2,*], Fei-fei Zhang[1,2,3], Jian-fei Xia[1], Na Sun[1], Guo-yu Shi[1],Yan-zhi Xia[1], Lin-hua Xia[1], Lu-chang Qin[4]*

[1] Laboratory of Fiber Materials and Modern Textile, the Growing Base for State Key Laboratory, College of Chemical and Environment Engineering, Shandong Sino-Japanese Center for Collaborative Research of Carbon Nanomaterials, Qingdao University, Qingdao, Shandong 266071, China;
[2] National Institute for Materials Science, Sengen 1-2-1, Tsukuba 305-0047, Japan
[3] Doctoral Program in Materials Science and Engineering, University of Tsukuba, 1-1-1 Tennodai, Tsukuba, 305-8577, Japan
[4] Department of Physics and Astronomy, University of North Carolina at Chapel Hill, Chapel Hill, NC 27599-3255, USA
[*]E-mail: wangzonghua@qdu.edu.cn; Tang.jie@nims.go.jp

The α-MnO$_2$ nanorods (MnO$_2$ NR) were first synthesized and then incorporated onto the basal plane of reduced graphene oxide (RGO) with the aid of ultrasonication to obtain a composite (MnO$_2$ NR/RGO). A novel modified electrode (MnO$_2$ NR/RGO/GCE) based on the MnO$_2$ NR/RGO composite was fabricated and used for the selective detection of uric acid (UA) in the mass of ascorbic acid (AA). The as-made modified electrode shows a good electron transfer ability and displays a novel performance for the detection of UA. More interestingly, this electrode can effectively eliminate the interference of AA. A linear dependence on the concentration of UA from $5 \times 10^{-8}$ to $4 \times 10^{-4}$ M was measured by differential pulse voltammetry (DPV), and the detection limit was up to $1 \times 10^{-8}$ M. The good sensitivity and repeatability of the proposed electrode enabled its successful application for the selective determination of UA in human urine sample analysis. These results will enhance our understanding of the applicability of MnO$_2$ NR/RGO in electrochemical analysis.

## 1. INTRODUCTION

Graphene, a two-dimensional (2D) monolayer of carbon atoms in a tightly packed honeycomb sp$^2$ carbon lattice, has attracted significant research interest in recent years. Its intriguing

physiochemical properties, such as unusual electric properties, large thermal conductivity, superior mechanical properties and chemical stability, large surface area, biocompatibility and electrochemical properties, provide potential applications in fabricating various electronic devices and biosensors [1-3]. Nowadays, graphene could be prepared by the facile route of the chemical reduction of graphene oxide with low cost, easy operation and mass production. More importantly, with their two-dimensional nanostructures and adjustable surface chemistry, graphene sheets can interact strongly with other organic and/or inorganic systems with combination and synergistic effects of different components [4-5]. Therefore, the special properties of graphene may provide insight for fabricating novel electrochemical sensors for virtual applications. Recently, graphene based modified electrodes have been reported extensively [6-7]. Compared with single walled carbon nanotubes, graphene illustrated a better sensitivity, signal-to-noise ratio, and stability. For example, Alwarappan et. al.[8] employed chemically synthesized graphene nanosheets as electrode materials for the electrochemical detection of important neurotransmitters such as dopamine and serotonin. Srivastava et al.[9] utilized functionalized multilayered graphene to immobilize urease and glutamate dehydrogenase for fabrication of a novel amperometric urea electrochemical biosensor with a lower detection limit of 3.9 mg/dL and a short response time of 10s. These enhanced sensing properties are mainly attributed to the presence of more $sp^2$-like planes and various edge defects present on the surface of graphene. Furthermore, several graphene composites, such as graphene/polymer composite, graphene/metal oxide composite and graphene/ionic liquid composite, based electrochemical sensors have also been developed for bioanalysis. For example, Shan et al.[10] constructed a novel polyvinylpyrrolidone-protected graphene/polyethylenimine-functionalized ionic liquid/glucose oxidase (GOD) composite electrochemical biosensor, achieving direct electron transfer of GOD. Palanisamy et al.[11] developed a nonenzymatic amperometric sensor for hydrogen peroxide using graphene oxide/zinc oxide composite by a simple and cost effective approach. Peng et al.[12] fabricated a graphene and room temperature ionic liquid (IL, $BMIMPF_6$) composite modified electrode towards the oxidation of azithromycin, obtaining a remarkably enhanced electrocatalytic activity. Sun et al.[13] constructed a graphene-$SnO_2$ nanocomposite modified electrode for the sensitive electrochemical detection of dopamine. In our previous work, we developed a quercetin-graphene composite-modified glassy carbon electrode (Qu/GH/GCE) for the selective and sensitive detection of dopamine (DA) [14]

Uric acid (UA) is a kind of small electroactive biomolecule, created when the body breaks down substances called purine nucleotides. High concentration of UA in blood leads to a type of arthritis, such as gout, and serum uric related to type II diabetes. The current detection methods of UA include enzymatic–based assay [15], capillary electrophoresis[16], high performance liquid chromatography[17] and electrochemical technique[18]. Among those methods, the electrochemical method is the most rapid, simple and convenient one. But one of the major problems in biological determination of uric acid comes from electrochemical interferences such as ascorbic acid (AA), which has a similar oxidation potential at normal electrodes. In order to solve this problem, various methods have been developed [19]. Recently, attention was paid to fabricating of carbon-based sensors for the detection of UA. For example, Alipour et al.[20] fabricated a pretreated pencil graphite electrode for the simultaneous determination of dopamine and uric acid in biological samples. Zhang et al.[21] reported simultaneous electrochemical determination of ascorbic acid, dopamine and uric acid with

helical carbon nanotubes. Sun et al.[22] created a graphene/Pt-modified glassy carbon electrode to simultaneously characterize AA, dopamine (DA), and UA levels. In this work, size-selected Pt nanoparticles with a mean diameter of 1.7 nm were self-assembled onto the graphene surface. In our previous work[23], for the purpose of selective determination of uric acid, we fabricated the poly acridine orange/graphene modified electrode (PAO/GH/GCE) by immobilizing graphene (GH) onto the surface of glassy carbon electrode (GCE), followed by electro-polymerizing acridine orange (AO) on the GH/GCE matrix with an electrolysis micelle disruption method.

Maganese oxides are a kind of attractive inorganic materials in biosensing application, due to their excellent catalytic oxidation abilities [24-26]. Recently, many efforts have been focused on the synthesis of nanoscale $MnO_2$/carbon-based materials (nanotubes, graphene, graphene oxide and porous carbon) hybrids due to their significant electrochemical applications, such as supercapacitors. Tang et al. [27] have successfully fabricated binderless supercapacitors using graphene and $MnO_2$-nanoflowers coated graphene. While a specific capacitance of 245 F/g was obtained for the graphene based supercapacitor, a much higher value of 328 F/g was reached for the capacitor based on $MnO_2$-coated graphene.

Herein, we fabricated a novel modified electrode based on $MnO_2$ nanorods ($MnO_2$ NR) and reduced graphene oxide (RGO) composite for the electrochemical detection of UA. The ultra large surface area of graphene provides more reactive sites for electroactive molecules, and its good conductivity can facilitate electron transfer. Thus, dramatical improvement in its sensitivity for UA is expected. Moreover, $MnO_2$ nanorods coated on the plane of graphene nanosheets could be as an eliminator of ascorbic acid and a separator for avoiding the restacking effect of graphene. The composites modified electrode may take advantage of the synergetic effect from graphene and $MnO_2$ nanorods and provide enhanced performance.

## 2. EXPERIMENTAL

### 2.1. Reagents and apparatus

Manganese sulfate ($MnSO_4$), $KMnO_4$, uric acid, KCl, L(+)–ascorbic acid and potassium hexacyanoferrate (III) ($K_3[Fe(CN)_6]$, $\geq$ 99.0%) were obtained from Nacalai tesque, Japan. Potassium hexacyanoferrate (II) trihydrate ($K_4[Fe(CN)_6]$, 98.5-102.0%) was purchased from Sigma-Aldrich. Graphite (99%) was provided by Nacalai tesque, Japan. Phosphate buffer solution (PBS) was prepared with 0.1 M $NaH_2PO_4$–$Na_2HPO_4$ and its pH was adjusted with $H_3PO_4$ or NaOH solutions. All aqueous solutions were prepared with Milli-Q water purified by a Millipore Milli-Q system (Millipore Japan).

Electrochemical experiments were performed via a CompactStat (Ivium Technologies, Netherlands) with a conventional three-electrode system at room temperature (25 ± 1°C). A bare electrode (glassy carbon electrode, GCE, 3 mm in diameter) and the modified electrodes were applied as working electrodes. A platinum wire was used as the counter. All the potentials quoted in this work were referred to a saturated calomel electrode (SCE) as the reference. All electrodes were purchased from BAS Inc., Japan.

Characterizations of morphologies and crystalline structure were performed by scanning electron microscopy (SEM, JSM-7001F), transmission electron microscopy (TEM, JEM-2100), atomic force microscopy (AFM, Agilent's PicoScan) and X-ray powder diffraction (XRD, RINT 2500HF, RIGAKU).

## 2.2. Synthesis of reduced graphene oxide (RGO)

Graphene oxide was synthesized by using the modified Hummers method. A mixture of graphite (3.0 g) and $NaNO_3$ (1.5 g) were added into 23 mL of 98% $H_2SO_4$, followed by stirring in an ice bath. After that, potassium permanganate ($KMnO_4$, 8.0 g) was then added to the suspension little by little. The mixture was stirred at room temperature for 2 h and then 90 mL of distilled water was added, which would be heated quickly to about 90°C. After being stirred for 12 h, 30 mL of 30 % $H_2O_2$ was added to the mixture. The mixture was washed by 5 % HCl and distilled water for several times for purification. After filtration and drying in vacuum, graphene oxide was obtained.

In a typical procedure for reduction of graphene oxide, graphene oxide (100 mg) was firstly dispersed in 30 mL distilled water and sonicated for 30 min. The brown graphene oxide (30 mL) suspension was mixed with 3 mL hydrazine monohydrate. The mixture was then put in a water bath (98°C) for 24 h. The stable black dispersion in the vial was washed with distilled water for several times to remove the excessive hydrazine and then centrifuged at 4000 rpm for 3 min to remove bulk graphite. The final product, RGO, was obtained by vacuum filtration and dried in vacuum.

## 2.3. Fabrication of modified electrode

A GCE was firstly polished by chamois leather containing $Al_2O_3$ slurry (first 0.3 μm then 0.05 μm), then ultrasonically cleaned in distilled water, finally dried at room temperature. 6 μL of RGO solution (1mg $mL^{-1}$) was dropped on the surface of GCE and dried in air to form the RGO modified electrode (RGO/GCE).

$MnO_2$ NR/RGO modified electrode ($MnO_2$ NR/RGO/GCE) was prepared by a simple casting method. Firstly, the $MnO_2$ nanorods ($MnO_2$ NR) were synthesized by hydrothermal method as the following processes: 0.2 g of manganese sulfate ($MnSO_4$) and 0.5 g of $KMnO_4$ were dissolved in deionized water (200 mL) under stirring. After that, the mixture was refluxed at 98°C for 6 h. Secondly, a mixture of $MnO_2$ NR and RGO at a concentration ratio of 1:1 (2 mg $mL^{-1}$ RGO and 2 mg $mL^{-1}$ $MnO_2$ NR) was dispersed in water and ultrasonicated to obtain well-proportioned composite solution. Finally, 6 μL of the composite solution (1mg $mL^{-1}$) was dropped onto a GCE and then dried at room temperature.

## 2.4. Electrochemical measurement

Electrochemical experiments were carried out in the three-electrode system by cyclic voltammetry (CV), differential pulse voltammetry (DPV) methods and electrochemical impedance

spectra (EIS). The potential interval of CVs was from -0.2 to 0.8 V, and the scan rate was selected as 100 mV/s. DPV conditions are: scan rate, 50 mV/s; amplitude, 10 mV; pulse width, 10 ms, with a potential interval from -0.2 to 0.8 V. The EIS measurements were performed under the open circuit potential with sinus amplitude of 5 mV at frequency ranges of 0.01Hz to 200kHz. Prior to each measurement, nitrogen ($N_2$) gas was bubbled directly into 10 mL of the cell solution for at least 15 min to obtain a $N_2$ -saturated solution, and during every measurement $N_2$ gas was flushed over the cell solution.

## 3. RESULTS AND DISCUSSION

### 3.1 Characterization of RGO, MnO₂ NR and MnO₂ NR/RGO composite

A TEM image of the as-synthesized RGO is shown in Fig. 1b. In this case, it clearly explains the flake-like shape. The morphology and nano-scale structure of graphene was further examined using atomic force microscope (AFM) shown in Fig.1a. From the Fig. 1a, it can be seen that the thickness of the RGO is about 2~3 nm, belonging to few-layer graphene given by the classification of the graphene-based nanomaterials[28].
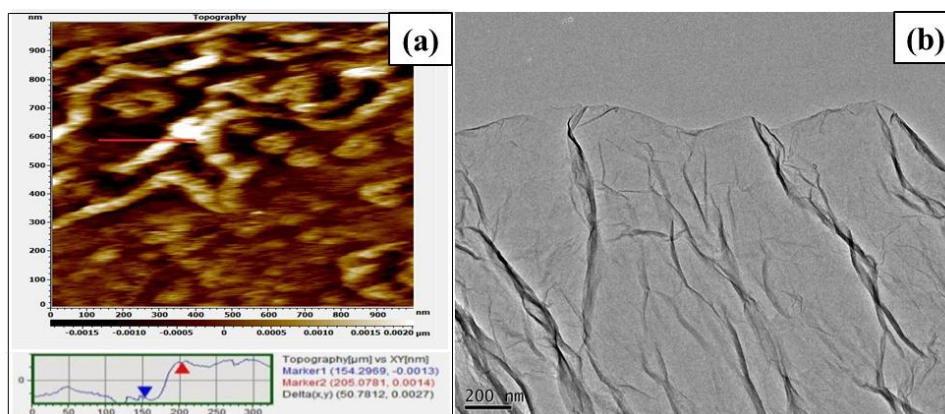


**Figure 1.** AFM (a) and TEM (b) images of as-prepared RGO.

The morphology of the $MnO_2$ and $MnO_2$ NR/RGO composite were presented in Fig. 2. Fig. 2 (a) is X-ray diffraction pattern of $MnO_2$. All the diffraction peaks can be easily indexed to planes of α-$MnO_2$ crystal, which are in agreement with the standard data file (JCPDS file NO. 42-1169). Fig. 2 (b) shows the TEM image of $MnO_2$. As shown, the as-synthesized $MnO_2$ looks like nanorods. The interplanar distance of $MnO_2$ (211,310) are 0.24 nm and 0.30 nm, respectively (Fig. 2 (b), inset). The morphologies of the as-synthesized $MnO_2$/graphene composite were illustrated in Fig. 2 (c, d). As revealed by the SEM and TEM images, the $MnO_2$ nanorods are randomly distributed on the surface of the RGO, which indicating the successfully formation of nanocomposites with graphene nanosheets and $MnO_2$ nanorods.
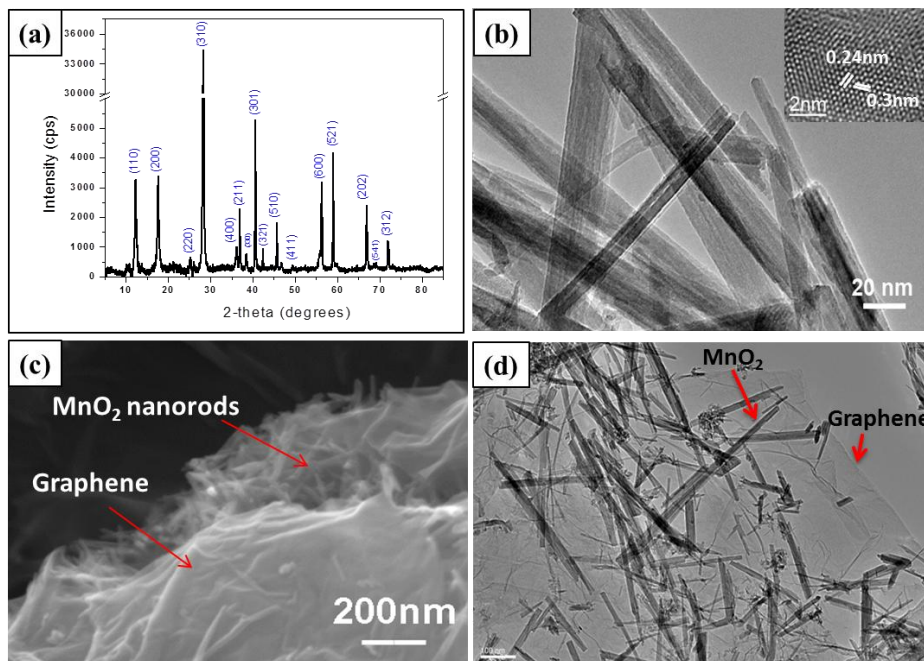
**Figure 2.** Morphology and structural characterization of as prepared $MnO_2$ and $MnO_2$/graphene composite. (a) XRD of $MnO_2$ nanorods, (b) TEM image of $MnO_2$ nanorods, the inset is a portion of the image at higher magnification, (c, d) SEM and TEM images of $MnO_2$/graphene composite.

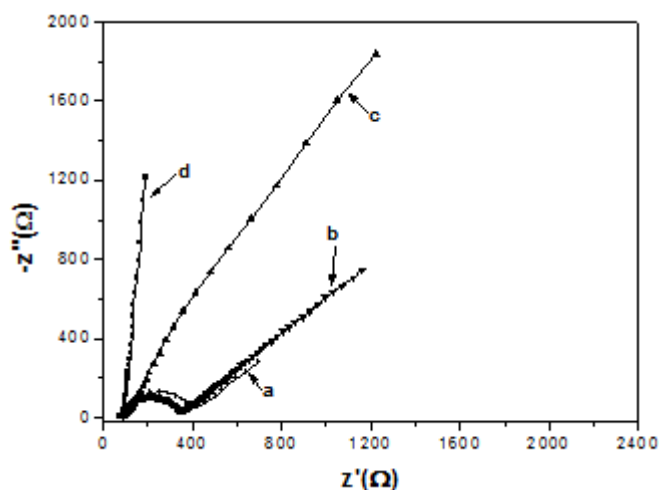*3.2. Electrochemical behaviors of the $MnO_2$ NR/RGO modified electrodes*



**Figure 3.** Electrochemical impedance spectra of the bare GCE (a), $MnO_2$ NR/GCE (b), $MnO_2$ NR /RGO/GCE (c) and GR/GCE (d) in 0.1 M KCl containing 3mM $[Fe(CN)_6]^{3-/4-}$. The frequency range is from 0.01Hz to 200 kHz. The amplitude of 5 mV was applied.

Electrochemical impedance spectrum (EIS) was applied for studying the performance of the electrode interface. Fig. 3 shows the electrochemical impedance spectra on the bare GCE (a), $MnO_2$

NR/GCE (b), MnO$_2$ NR/RGO/GCE (c) and RGO/GCE (d) in 0.1M KCl containing equimolar [Fe(CN)$_6$]$^{3-/4-}$. As shown, the electron transfer resistance of the electrode decreased after modification, and compared to RGO/GCE, the modification of graphene with MnO$_2$ inhibits fast electron transfer to some extent due to the presence of semiconductive MnO$_2$. Nevertheless, the Nyquist complex plane plot of MnO$_2$ NR/RGO/GCE is almost straight line, which shows that the MnO$_2$ NR/RGO/GCE still keeps fast electron transfer.

The DPV responses of the mixture solution containing 0.5mM UA and 0.5mM AA at the different modified electrodes are shown in Fig. 4 (A). As shown, UA and AA exhibited an overlapped and broad anodic peak at bare GCE (a) with a peak potential at 375 mV. Two oxidation peaks of UA and AA at the RGO/GCE (c) were observed at 300 mV and -10 mV, respectively. However, only the oxidation peak of UA at MnO$_2$ NR/GCE (b) and MnO$_2$ NR/RGO/GCE (d) was obtained at 310 mV and 335 mV respectively, which indicates that MnO$_2$ NR can eliminate the oxidation of AA. Compared with some reported electrode [29, 30], our modified electrode can completely avoid the interferent of AA.

It also shows that the oxidation current of UA at MnO$_2$ NR/RGO/GCE is dramatically increase by 14 times compared to the MnO$_2$ NR/GCE. This because RGO could provide more reactive sites for UA molecules, and help to realize fast electron transfer between electrode and UA.
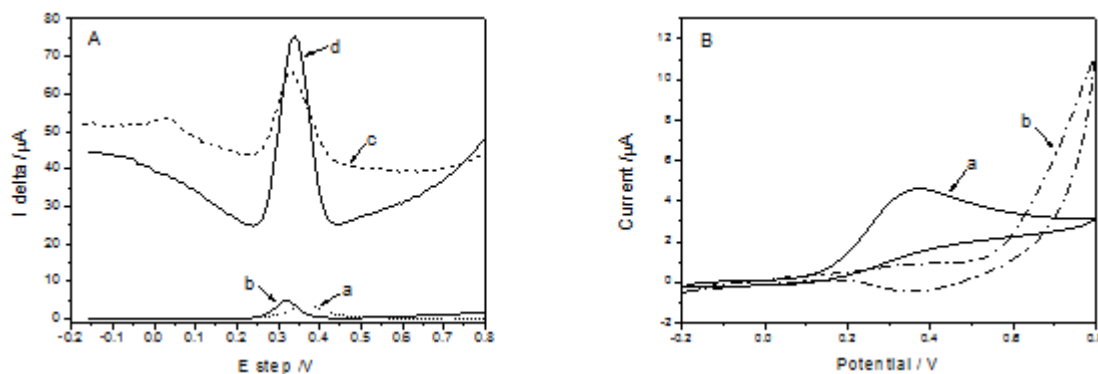


**Figure 4.** (A) DPVs of the bare GCE (a), MnO$_2$ NR/GCE (b), RGO/GCE (c), MnO$_2$ NR/RGO/GCE (d) in PBS (pH 6.5) containing a mixture of 0.5 mM UA and 0.5 mM AA in PBS (pH 6.5). DPV conditions: scan rate, 50 mV/s; amplitude, 10 mV; pulse width, 10 ms. (B) Current responses of 0.1 mM AA at bare GCE (a) and MnO$_2$ NR /GCE (b) in 0.1M pH 6.5 PBS. Scan rate: 100 mV/s.

In order to verify the mechanism of eliminating effect of AA at MnO$_2$ NR/GCE, the CV responses of 1.0 mM AA on the bare GCE and the MnO$_2$ NR/GCE in 0.1M pH 6.5 PBS were studied. Fig. 4 (B) shows there is a big respond of AA at the bare GCE with the peak current of $6\times10^{-7}$ A (curve a ), whereas there is no current respond of AA at the MnO$_2$ NR/GCE (curve b), indicating MnO$_2$ NR can eliminate the effect of AA. This may arise from a special reaction that MnO$_2$ can catalyze hydroxyl to carbonyl, and this carbonyl form has no-electrochemical activity. The special reaction is illustrated as below. MnO$_2$ nanoparticles has been reported that can electively oxidize AA to

electrochemical inactive product, and thus eliminate the interference of AA on a glucose biosensor [31].
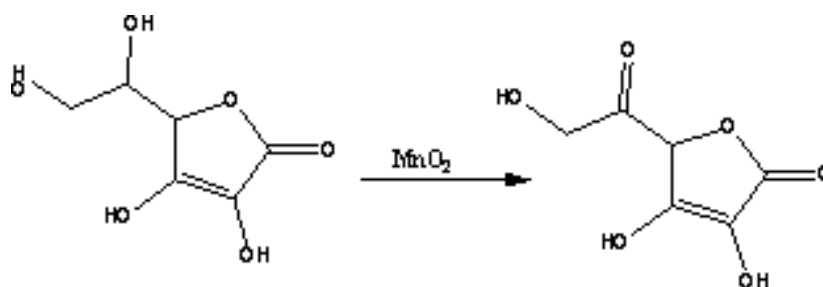


Moreover, we studied the effect of the scan rates from 10 to 300 mV/s on the electrochemical behavior of UA at the $MnO_2$ NR/RGO/GCE. A relationship between the peak current and the scan rate is linear with the scan rate increased from 20 to 250 mV/s. The equation is $I_p$ (μA) = 33.26 + 0.79 $v$ (mV/s), R = 0.9923, indicating that the electrochemical oxidation of UA at the $MnO_2$ NR/RGO/GCE was controlled by adsorption process.

### 3.3. UA Electrochemical detection performance on the MnO₂ NR/RGO/GCE

Under the optimal conditions, the $MnO_2$ NR/RGO/GCE was applied for UA detection. The dependence of the peak current response on UA concentration is shown in Fig. 5. The anodic peak current response showed a linear increase as the UA concentration increased from $5 \times 10^{-8}$ to $4 \times 10^{-4}$ M. The regression equation is $I_p$ (μA) = 6.89 + 0.17 C (μM) (R= 0.9992) and the detection limit is up to $1.0 \times 10^{-8}$ M (S/N = 3).
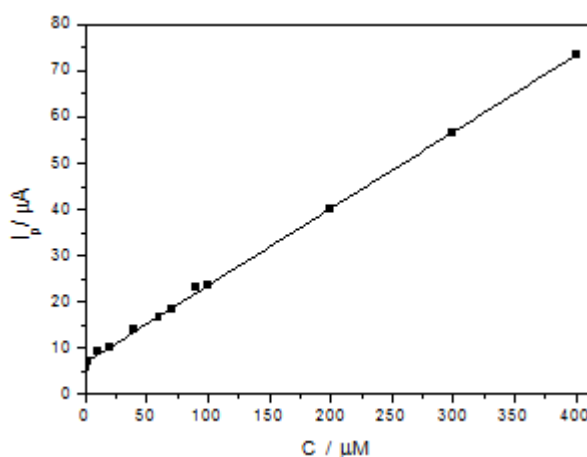


**Figure 5.** The linear relationship between the peak current and UA concentration from $5 \times 10^{-8}$ to $4 \times 10^{-4}$ M in 0.1M pH 6.5 PBS.

Compared with some reported modified electrode [32, 33], the analytical performances of the proposed electrode have wider linear range and lower detection limit. In addition, the modified electrode showed good stability and reproducibility. A relative standard deviation (RSD) is 1.8 % for

20 times parallel detections of 0.1 mM UA. In order to understand the stability of the modified electrode, it was stored at room temperature for four weeks. 95.5% of the initial response current was remained after four weeks. Therefore, the MnO$_2$ NR/RGO/GCE displays the promise for the determination of UA with high sensitivity, low detection limit and good reproducibility.

### 3.4. Analysis of human urine samples

The MnO$_2$ NR/RGO/GCE was applied to the direct analysis of UA in human urine samples. The urine samples were acquired from our three laboratory person and then diluted by using 0.1 M PBS for determination (1000 times dilution of the 24-hour collected urine sample). The results obtained from five parallel measurements were presented at Table 1. The recovery by standard additions method and RSD confirmed that proposed method can be used effectively for the quantitative analysis of UA.

**Table 1.** Analysis of UA in human urine ($n = 5$)

| Sample | UA determined (μM) | UA added (μM) | Found (μM) | Recovery (%) | RSD (%) |
|--------|--------------------|---------------|-----------|--------------|---------|
| Urine 1 | 1.98 | 10 | 12.01 | 100.2 | 1.2 |
| Urine 2 | 2.00 | 20 | 21.68 | 98.5 | 1.6 |
| Urine 3 | 2.03 | 30 | 32.25 | 100.6 | 1.3 |

## 4. CONCLUSIONS

A novel modified electrode MnO$_2$ NR/RGO/GCE was fabricated by using synthesized MnO$_2$ NR/RGO film and then used to investigate the electrochemical behavior of UA in the presence of AA. The MnO$_2$ nanorods could eliminate the effect of AA effectively. Moreover, ultra large surface area and good conductivity of RGO can provide more reactive sites for UA molecules and help to realize fast electron transfer. The higher selectivity and sensitivity towards UA were acquired at MnO$_2$ NR/RGO/GCE. The developed modified electrode has been applied to the determination of UA in human urine with satisfactory results.

**References**

1.  Z. H. Wang, C. F. Zhou, J. F. Xia, B. Via, Y. Z. Xia,  F. F. Zhang, Y. H. Li, L. H. Xia. *Colloid Surface B*, 106 (2013) 60.

2.   Y. Wang, J. Lu, L. Tang, H. Chang, J. Li, *Anal. Chem.*, 81 (2009) 9710.
3.   D. Chen, H. Feng, J. Li, *Chem. Rev.*, 112 (2012) 6027.
4.   A. A. Elzatahry, A. M. Abdullah, T. A. S. El-Din, A. M. Al-Enizi, A. A. Maarouf, A. Galal, H. K. Hassan, E. H. El-Ads, S. S. Al-Theyab and A. A Al-Ghamdi. *Int. J. Electrochem. Sci*., 7 (2012) 3115.
5.   Z. H. Wang, J. F. Xia, X. M. Guo, Y. Z. Xia, S. Y. Yao, F. F. Zhang, Y. H. Li, L.H. Xia., *Anal. Methods*, 5 (2013) 483.
6.   Z. H. Wang, Y. L. Gao, J. F. Xia, F. F. Zhang, Y. Z. Xia, Y. H. Li, *C. R. CHIM*., 15 (2012) 708.
7.   Y. Shao, J. Wang, H. Wu, J. Liu, I.A. Aksay, Y. Lin, *Electroanal.*, 22 (2010) 1027.
8.   S. Alwarappan, A. Erdem, C. Liu, C. Z. Li, *J. Phys. Chem. C* 113 (2009) 8853.
9.   R.K. Srivastava, S. Srivastava, T.N. Narayanan, B.D. Mahlotra, R. Vajtai, P.M. Ajayan, A. Srivastava, *ACS Nano*, 6 (2012) 168.
10.  C.S. Shan, H.F. Yang, J.F. Song, D.X. Han, A. Ivaska, L. Niu, *Anal. Chem.*, 81 (2009) 2378.
11.  S. Palanisamy, S.M. Chen, R. Sarawathi, *Sensor Actuat. B-Chem*., 166 (2012) 372.
12.  J.Y. Peng, C.T. Hou, X.X. Liu, H.B. Li, X.Y. Hu, *Talanta,* 86 (2011) 227.
13.  W. Sun, X. Wang, Y. Wang, X. Ju, L. Xu, G. Li, Z. Sun, *Electrochim. Acta*, 87 (2013) 317.
14.  Z. H. Wang, J. F. Xia, L. Y. Zhu, X. Y. Chen, F. F. Zhang, S.Y. Yao, Y. H. Li, Y. Z. Xia, *Electroanal.*, 23 (2011) 2463.
15.  N.C.M. Zanon, O.N. Oliveira, L. Caseli, *J. Colloid. Interf. Sci.*, 373 (2012) 69.
16.  C.D. Georgakopoulos, F.N. Lamari, I.N. Karathanasopoulou, V.S. Gartaganis, N.M. Pharmakakis, N.K. Karamanos, *Biomed. Chromatogr.* 24 (2010) 852.
17.  Y. G. Zuo, C. J. Wang, J. P. Zhou, A. Sachdeva, V. C. Ruelos, *Anal. Sci,.* 24 (2008) 1589.
18.  T. H. Tsai, Y. C. Huang, S. M. Chen, M. A. Ali, F. M. A. AlHemaid, *Int. J. Electrochem. Sci.*, 6 (2011) 6456
19.  Z. H. Wang, Y. M. Wang, G. A. Luo, *Analyst*, 127 (2002) 1353.
20.  E. Alipour, M.R. Majidi, A. Saadatirad, S.m. Golabi, A.M. Alizadeh, *Electrochim. Acta,* 91 (2013) 36.
21.  B. Zhang, D. Huang, X. Xu, G. Alemu, Y. Zhang, F. Zhan, Y. Shen, M. Wang, *Electrochim. Acta,* 91 (2013) 261.
22.  C. L. Sun, H. H. Lee, J. M. Yang, C. C. Wu, *Biosens. Bioelectron.*, 26 (2011) 3450.
23.  Z. H. Wang, J. F. Xia, L. Y. Zhu, F. F. Zhang, X. M. Guo, Y. H. Li, Y. Z. Xia, *Sensor Actuat. B-Chem.*161 (2012) 131.
24.  Z. Y. Wu, S. Thiagarajan, S. M. Chen, K. C. Lin, *Int. J. Electrochem. Sci.,* 7 (2012) 1230
25.  A. Samphao, H. Rerkchai, J. Jitcharoen, D. Nacapricha and K. Kalcher, *Int. J. Electrochem. Sci.*, 7 (2012) 1001.
26.  L. Y. Shao, J. Shu, R. Ma, M. Shui, L. Hou, K. Q. Wu, D. J. Wang, Y. L. Ren, *Int. J. Electrochem. Sci*., 8 (2013) 1170.
27.  Q. Cheng, J. Tang, J. Ma, H. Zhang, N. Shinya, L. C. Qin, *Carbon*, 49 (2011) 2917.
28.  C.N.R. Rao, A.K. Sood, K.S. Subrahmanyam, A. Govindaraj, *Angew. Chem. Int. Edit.*, 48 (2009) 7752.
29.  M. Sadikoglu, G. Taskin, F. G. Demirtas, B. Selvi, M. Barut, *Int. J. Electrochem. Sci.,* 7 (2012) 11550 .
30.  X. B. Li, G.R. Xu, R. Y. Hu, *Int. J. Electrochem. Sci.*, 8 (2013) 1920
31.  J. J. Xu, X. L. Luo, Y. Du, H. Y. Chen, *Electrochem. Commun.*, 6 (2004) 1169.
32.  T. Nie, L. M. Lu, L. Bai, J. K. Xu, K. X. Zhang, O. Zhang,  Y. P. Wen, L. P. Wu, *Int. J. Electrochem. Sci.,* 8 (2013) 7016.
33.  C. Y. Wang, F. C. Ye, H.F. Wu, Y. Qian, *Int. J. Electrochem. Sci.*, 8 (2013) 2440.